第10卷 第8期
1990年8月
光 学 学 报
ACTA OPTICA SINICA
Vol. 10, No. 8
August, 1990

Analyses of Optical Resonator for Continuous Wave Mode-Locked Neodymium: Phosphate Glass Laser

J. D. Ling, L. Yan and Chi H. Lee
(Department of Electrical Engineering, University of Maryland, U. S. A.)
(College Park, Maryland 20742)

Abstract

Continuous wave mode-locked neodymium phosphate glass laser requires special resonator design since Nd: phosphate glass has low thermal conductivity and damage threshold. We analyze the characteristics of a three-element resonator under the restraint of a fixed resonator length and discuss the design of the optical resonator for the CW actively mode-locked Nd: phosphate glass laser. We discuss the stability ranges and characteristics of resonator under different parameter regions and illustrate the best parameter region of interest. Analytical expressions of resonator parameters for optimum operation regime are given. The experimental results agree well with theoretical predictions. This. analysis may be useful for the design of any end-pumped and mode-locked resonator with three elements or more elements.

Key words: Nd: phosphate glass laser; three-element resonator; actively mode-locked laser.

I. Introduction

Since the invention of the laser, numerous optical resonators have been designed to accommodate various needs, and many theoretical analyses of optical resonators have been made[1~6]. The continuous wave, actively mode-locked neodymium (Nd) phosphate glass laser has its own resonator design requirements. Since Nd: phosphate glass has low thermal conductivity and damage threshold, the conventional, flash lamp pumped Nd: glass laser can only operate at a repetition rate of a few hertz. A continuous wave (CW) operation of Nd: phosphate glass laser requires focussing relatively low power, narrow band pump light into a small region. By employing the longitudinal pumping scheme, the CW actively mode-locked Nd: phosphate glass laser has been realized[7] and short picosecond pulses have been produced[8].

For such longitudinal pumping scheme, the pump beam has to be focused to a beam diameter of around 100μm. To maximize the effective gain for a given pump power, the intracavity laser beam size at the active medium should be about the same as that of the pumping beam and the active medium is preferably near one end of the optical resonator for a convenient delivery of the pumping beam. In addition, it is desirable that the resonator characteristics are not sensitive to the adjustment of the

Received 16 February, 1990.

resonator length.

We chose a three-element optical resonator which consists of two end mirrors and a focusing element (an intracavity thin lens for the transmitting type[3] or a concave mirror for the reflecting type[4]. Such type of resonator had been employed in dye laser[9] and analyzed[3], where the total resonator length may be varied. In the case of an actively mode-locked laser, the total resonator length is fixed in order to match the frequency of the mode-locker. In this paper, we will analyze the characteristics of the three-element resonator under the restraint of a fixed resonator length and discuss the design of the optical resonator for the CW actively mode-locked Nd: phosphate glass laser.

The simplest three-element resonator is formed by inserting a thin focusing lens into a plane-parallel resonator, as shown in Fig. 1. It is referred to as the linear resonator. The two beam waists fall on the two end mirrors. Since the two waists are generally not equal in size, the linear resonator will have a left-right asymmetry of beam divergence. On the left hand side of the lens the wave fronts bend toward the left. By passing through the lens the wave fronts bend toward the right. We may consider that they are the conjunction of two plana-spherical resonators by the link of a lens[10,11]. Each of them has its own waist and semiconfocal length. In section II we will discuss the stability ranges and characteristics of the linear resonator under different parameter regions and then illustrate the best parameter region of interest. In section III, some experimental data of the linear resonator are presented and compared with the theoretical calculations. In section IV the linear resonater is compared with the hemispherical resonator[5]. In section V analyses of the basic three element resonator (linear resonator) are applied to some other variant resonators, such as a linear resonator ending with concave mirror, a folded resonator and a ring resonator. Except for the ring resonator they are all three element resonators. Astigmatism ard thermal lensing effect are not included in this paper.

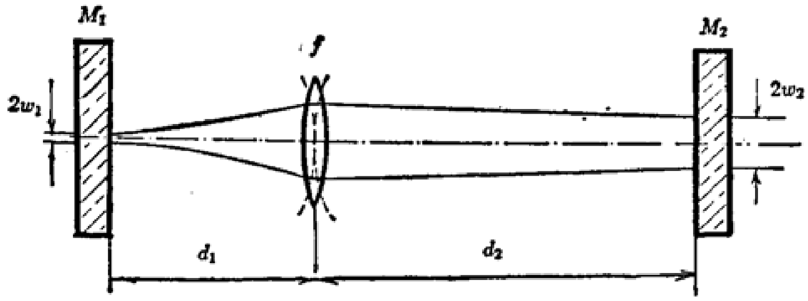

Fig. 1 Schematic of plane-parallel resonator with thin lens f, $2w_1$-laser beam waist on the plane mirror M_1, $2w_2$-beam waist on the plane mirror M_2

II. Analysis and Characteristics of Linear Resonator

Analytical Expressions

To analyze the characteristics of the linear resonator we employ the standard matrix method dealing with the fundamental gaussian beam propagation[1,12]. For a gaussian beam, it is clear that there are two beam waits at each plane mirror. Since the beam waist size and its location are the basic parameters of an optical resonator, we choose the reference plane at the mirror M_1. The round trip ABCD matrix is then given by

$$\begin{pmatrix} A_1 & B_1 \\ C_1 & D_1 \end{pmatrix} = \begin{pmatrix} 1 & d_1 \\ 0 & 1 \end{pmatrix} \begin{pmatrix} 1 & 0 \\ -\frac{1}{f} & 1 \end{pmatrix} \begin{pmatrix} 1 & 2d_2 \\ 0 & 1 \end{pmatrix} \begin{pmatrix} 1 & 0 \\ -\frac{1}{f} & 1 \end{pmatrix} \begin{pmatrix} 1 & d_1 \\ 0 & 1 \end{pmatrix}$$

$$= \begin{pmatrix} 1-\frac{2(d_1+d_2)}{f}+\frac{2d_1 d_2}{f^2} & 2(d_1+d_2)-4\frac{d_1 d_2}{f}-\frac{2d_1^2}{f}+\frac{2d_1^2 d_2}{f^2} \\ -\frac{2}{f}\left(1-\frac{d_2}{f}\right) & 1-\frac{2(d_1+d_2)}{f}+\frac{2d_1 d_2}{f^2} \end{pmatrix}. \tag{1}$$

The condition for a stable resonator is

$$-1 \leqslant \frac{1}{2}(A_1+D_1) \leqslant 1. \tag{2}$$

The radius of curvature R_1 and the beam waist size w_1 at the reference plane are

$$R_1 = \frac{2B_1}{D_1 - A_1}, \tag{3}$$

$$w_1 = \left(\frac{\lambda}{\pi n}\right)^{1/2} \frac{|B_1|^{1/2}}{\left[1-\left(\frac{D_1+A_1}{2}\right)^2\right]^{1/4}}. \tag{4}$$

The corresponding angle of divergence is

$$\theta_1 = \frac{\lambda}{\pi w_1 n}, \quad n=1. \tag{5}$$

The expressions of A_1, D_1 and B_1 at the reference plane of M_1 are

$$A_1 = D_1 = 1-\frac{2(d_1+d_2)}{f}+\frac{2d_1 d_2}{f^2}, \tag{6}$$

$$B_1 = 2(d_1+d_2)-\frac{4d_1 d_2}{f}-\frac{2d_1^2}{f}+\frac{2d_1^2 d_2}{f^2}. \tag{7}$$

Substituting Eq. (6) into Eq. (2) we obtain the stability condition:

$$0 \leqslant \left(1-\frac{d_1}{f}\right)\left(1-\frac{d_2}{f}\right) \leqslant 1. \tag{8}$$

It is an equi-hyperbola on $\left(1-\frac{d_1}{f}\right)$ and $\left(1-\frac{d_2}{f}\right)$ coordinates plane, as shown in Fig. 2. It is clear that for a stable resonator, either both d_1 and d_2 must be smaller than f (region in the first quadrant) or both d_1 and d_2 must be larger than f (region in the third quadrant). The different characteristics of both cases will be discussed latsr. Because of the symmetry, the corresponding results for the beam waist ω_2 at the mirror M_2 can be easily obtained by interchanging d_1 and d_2 in Eqs. (6) ~ (7).

We mention hero that in a real resonator, there are some intracavity elements such as the gain medium. d_1 is related to the physical distance d_{1phys} by

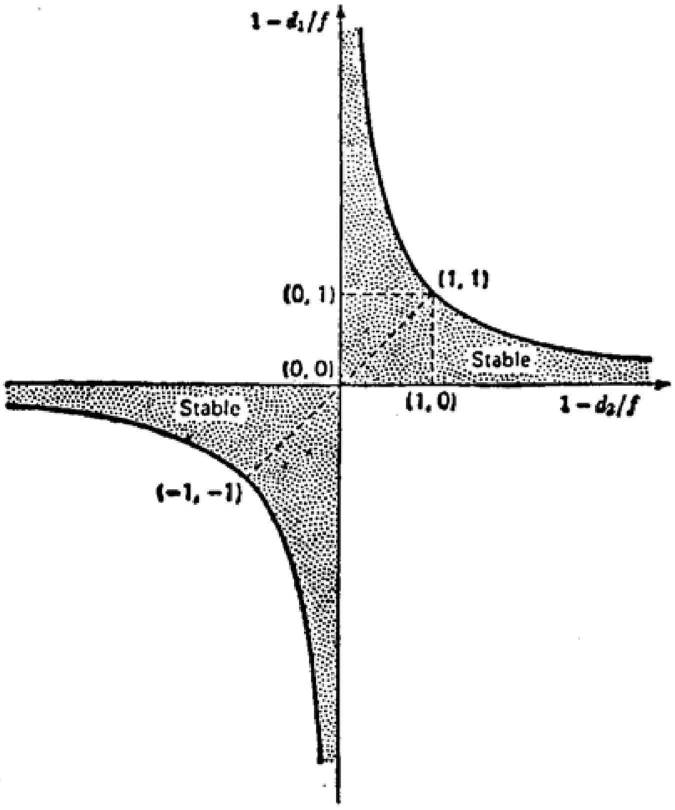

Fig. 2 Stability diagram for the thin lens resonator, modified from ref. [14], "Solid State Laser Engineering"

$$d_1=D_{1\mathrm{Phys}}-l_1\left(1-\frac{1}{n_1}\right) \tag{9}$$

where l_1 and n_1 are the length and index of refraction of the gain medium between mirror M_1 and the intracavity thin lens. The total cavity length

$$d_0=d_1+d_2. \tag{10}$$

Likewise, d_2 is related to the physical length $d_{2\mathrm{Phys}}$ similarly as (9). The total resonator length d_0 differs from the physica resonator length by

$$d_0=d_{1\mathrm{Phys}}-l_1\left(1-\frac{1}{n_1}\right)-l_2\left(1-\frac{1}{n_2}\right) \tag{11}$$

Characteristics of the Optical Resonator

In an actively mode-locked laser, the total cavity length d_0 is fixed, and the focal length of the thin lens is also constantl once the lens is chosen. We choose $d_0=150$ cm as it is one of the convenient cavity lengths, to match the frequency of the mode-locker.

i) Linear resonator in the third quadrant

We first consider both d_1 and $d_2>f$, so the resonator is in the region of the third quadrant of Fig. 2. It is required that

$$f<d_0/2. \tag{12}$$

The resonator stable range is, from Eq. (8), given by

$$f<d_1<\frac{d_0}{2}\left(1-\sqrt{1-4\frac{f}{d_0}}\right). \tag{13}$$

The resonator stability range is defined and obtained as

$$d_s=d_{1\max}-d_{1\min}$$
$$=\frac{d_0}{2}\left(1-\sqrt{1-4\frac{f}{d_0}}\right)-f. \tag{14}$$

For a resonator length $d_0=150$ cm and focal length $f=15$ cm, d_s is 1.92 cm, a fairly large range.

Fig. 3 shows the two beam waist sizes w_1 and w_2 as d_1 varies, with different f as parameters. Near the middle of the stable range, is at a maximum and w_2 has an inflection. It is clear that by adjusting d_1 near the middle of the stablo range, there

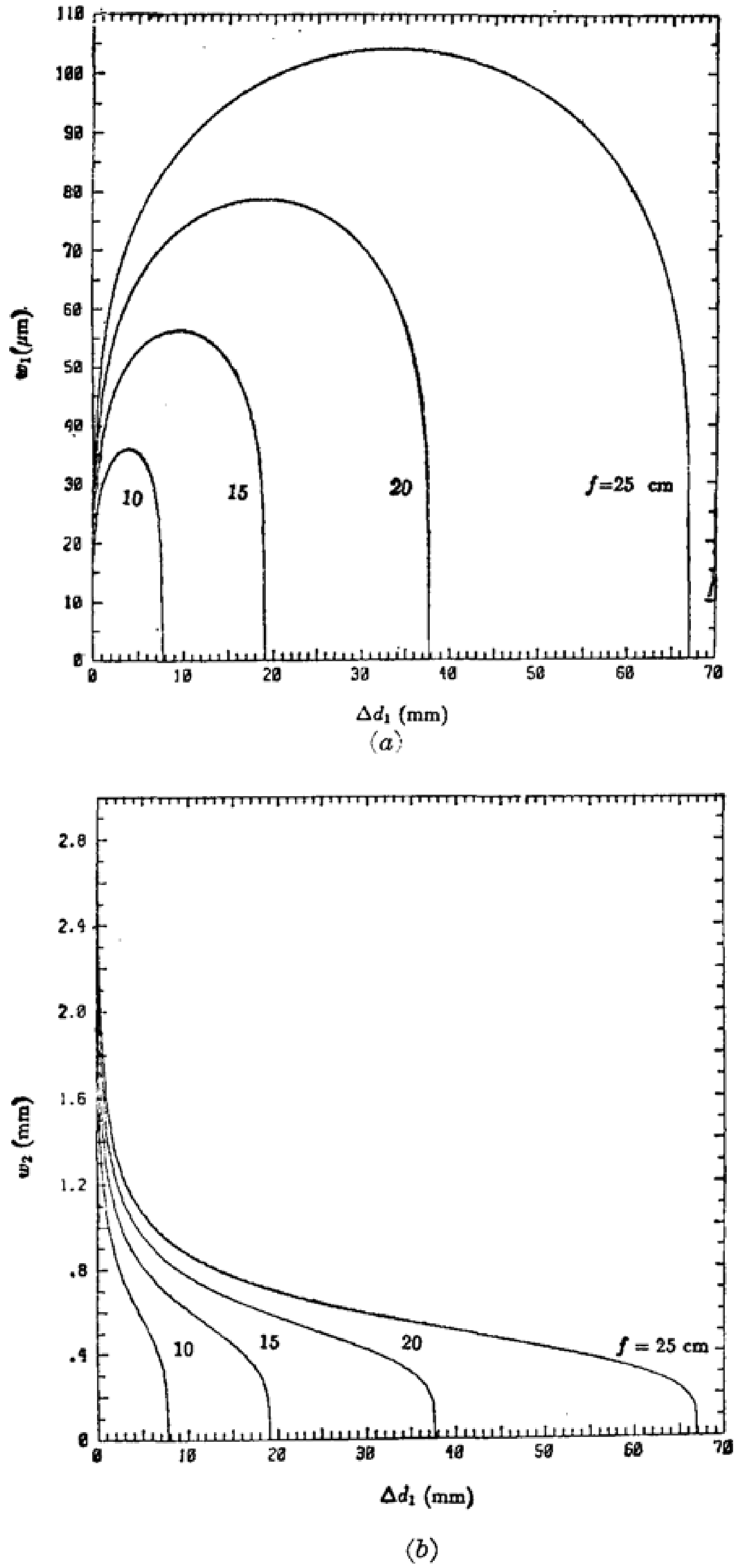

Fig .3　Characteristics of the linear resonator in the third quadrant of stability, $f<d_1$ and d_2, $d_0=d_1+d_2=150$cm $\Delta d_1=d_1-f$

(a) Variations of the smaller beam waist size w_1 vs. Δd_1;

(b) Variations of the larger beam waist size w_2 vs. Δd_1

will be least changes in w_1 and w_2 due to a small change of d_1 and/or d_2. For the chosen focal lengths, the maximum of w_1 ranges from 36 to 104 μm which are the practical beam sizes with the longitudinal pumping by another laser. Thus, the active medium can be located near the smaller beam waist of size w_1. The size of the larger beam waist, w_2, is of a magnitude around 600 μm. This beam waist is located at the mirror M_2 which is used as the output coupler. Hence, the output laser beam divergence is small (full divergence angle $\theta \simeq 1.1$ mrad) even though one needs a very small beam size at the active medium. By adjusting d_1 slightly smaller than the middle of the stable range, even larger w_2, consequently smaller beam divergence can be obtained.

ii) Analytical formulas for calculation of optimum operation regime in the third quadrant

From above analyses, we know that for a given resonator length d_0, there is an optimum value d_{10} for the distance d_1 which results in a maximum beam waits ω_{1max}. We can obtain analytical expressions of d_{10} and ω_{1max} in the following way. We first remove the restraint of a fixed resonator length and treat d_1 and d_2 as independent parameters. There is still a stable range for d_1:

$$f < d_1 < f + d_s' \tag{15}$$

where d_s', from Eq. (8), is given by

$$d_s' = \frac{f^2}{d_2 - f}. \tag{16}$$

Using Eqs. (4), (6) ~ (7) and (16), it can be shown that when d_1 is exactly at the middle of the stable range

$$d_{10} = f + \frac{1}{2} d_s', \tag{17}$$

the stability parameter $\frac{1}{2}(A+D) = 0$ and the small beam waist size w_1 has a maximum value w_{1max} given by

$$w_{1max} = \left(\frac{\pi d_s'}{2\pi n}\right)^{1/2}. \tag{18}$$

Combining Eq. (16) and (17), the optimum d_1 can be written as

$$d_{10} = f\left(1 + \frac{f}{2(d_2 - f)}\right). \tag{19}$$

Eqs. (16), (18) and (19) can be used in calculations of resonator parameters for a given d_2 and f.

Now suppose we want to choose d_2 such that

$$d_0 = d_{10} + d_2 \tag{20}$$

is a desired resonator length. Combining Eqs. (19) and (20), we find

$$d_{10} = \frac{d_0 - \sqrt{d_0^2 - 2f(2d_0 - D)}}{2} \tag{21}$$

Using Eq. (16), w_{1max} can be rewritten as

$$w_{1\,max} = \left(\frac{\lambda(d_{10} - f)}{\pi n}\right)^{1/2} \tag{22}$$

Eqs. (21) and (22) can be used in calculations of resonator parameters for a given d_0 and f. We should note that the detailed resonator characteristics such as stable range are slightly different in the situations of fixed d_0 or fixed d_2. However, w_{1max} occurs only in a particular point of the stable range. This point (d_{10}, w_{1max}) is the same for fixed d_0 or fixed d_2 which "happens" to give $d_{10}+d_2=d_0$. This is why d_{10} and w_{1max}, in the situation of fixed d_0, can be calculated in a different way as by Eqs. (21) and (22).

In the situation of active mode-locking, the resonator length usually needs a fine adjustment to match the (acoustooptic) modulator's frequency which is tuned to the (acoustic) resonant frequency. This can be done by adjusting d_2. We can now estimate the effect of changing d_2 upon d_{10}. For a fixed f, we obtain, from Eq. (19),

$$\Delta d_{10}=-\frac{f^2}{2(d_2-f)^2}\Delta d_2. \tag{23}$$

Since usually $d_2\gg f$, the effect of changing d_2 upon d_{10} is reduced greatly. For a typical $f=15$ cm and d_2 about $100\sim135$ cm, the reducing factor is 10^{-2}. Hence, for $\Delta d_2=20$ cm, Δd_{10} is only about 2 mm. And from Fig. 3 we see that even if d_1 is kept at the original d_{10}, the corresponding change of w_1 due to a shift Δd_{10} is very small. Therefore, some change of d_2 will not severely affect the resonator characteristics. Since d_2 accounts for a much larger portion of the total resonator length d_0, the flexibility of d_2 reflects the flexibility of d_0.

We then look at the effect of changing d_0, the total resonaor length, or f, the focal length of the thin lens, upon the maximum small beam waist size w_{1max}. Fig. 4a shows that w_{1max} decreases with increasing of d_0 when f is kept constant at 15 cm. We see that the variation of w_{1max} is very smooth. w_{1max} is changed less than 5 μm by changing 20 cm of the total resoator length. Such characteristic is very useful as it greatly facilitates the adjustment of d_0 even by quite a large amount. On the other hand, in contrast to d_0, f strongly affects the value of w_{1max}. As shown in Fig. 4b, w_{1max} increases with f almost linearly when d_0 is kept at constant 150 cm. However, over a reasonable range of f, w_{1max} can change by a factor of three. Such a strong dependence of w_{1max} on f is also a nice property since it allows one to easily obtain, over a large range, a desirable beam waist size by choosing a proper and yet practically available thin lens.

iii) Linear resonator in the first quadrant

We then consider the case where d_1 and $d_2<f$, namely the region of the first quadrant in Fig. 2. Clearly, the focal length f of the thin lens must be larger than $\frac{1}{2}d_0$ for a stable resonator. From Eq. (8), the range of d_1 in which the resonator is stable is given by

$$d_0-f<d_1<f. \tag{24}$$

If $f\geqslant d_0$, we have

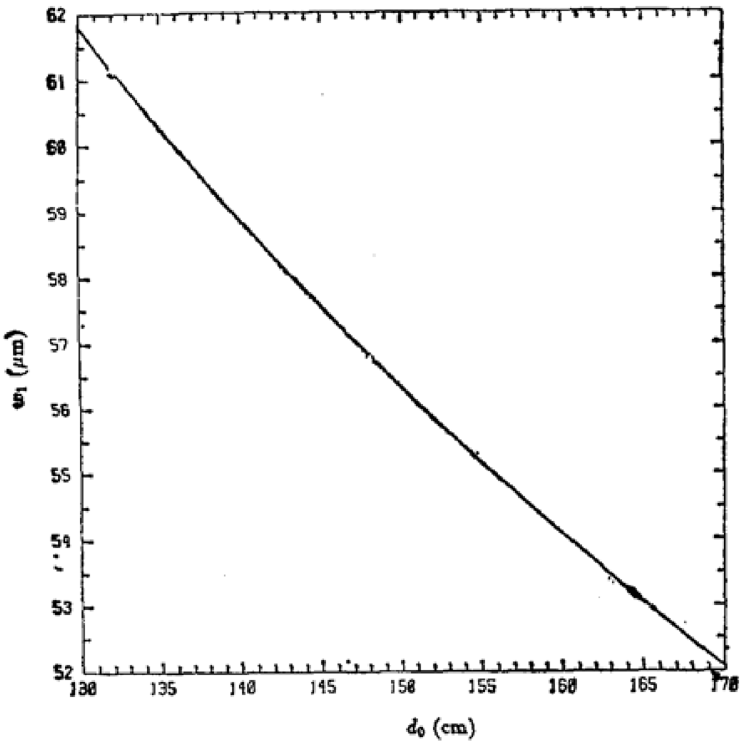

(c)

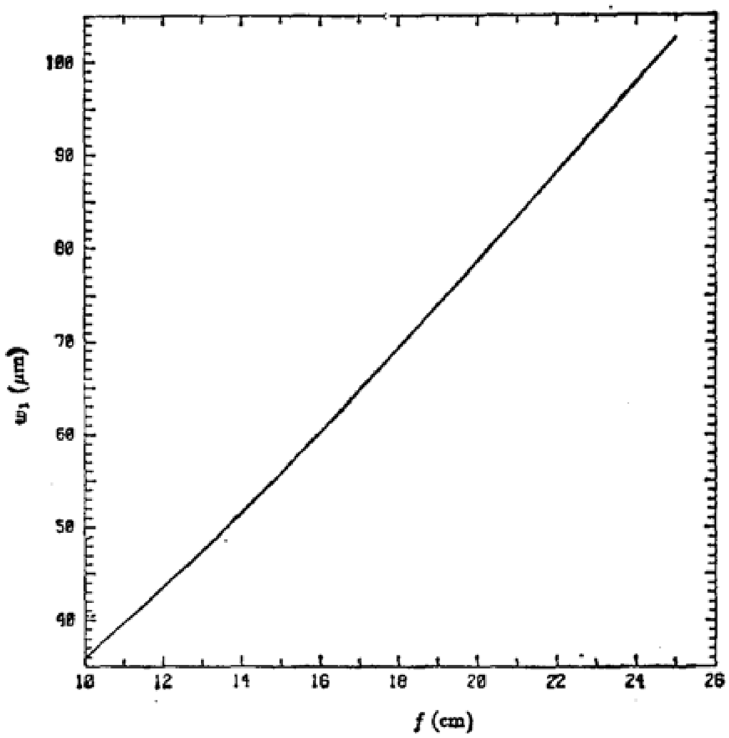

(b)

Fig. 4 The effect of changing the focal length f or the resonator length d_0 on the maximum beam waist size w_{1max} of the linear resonator in the third quadrant of stability

(a) The effect of changing d_0 on w_{1max}, $f=15$ cm;

(b) The effect of changing f on w_{1max}, $d_0=150$ cm

$$0<d_1<d_0, \tag{25}$$

so the optical resonator is always stable regardless of the intracavity position of the thin lens. In Fig. 5, the beam waist size w_1 are plotted as d_1 varies, with f as a parameter. Since the variation range of the thin lens position, from Eq. (24), is symmetrical about the $\frac{1}{2}d_0$ point, the two beam waist sizes w_1 and w_2 interchange

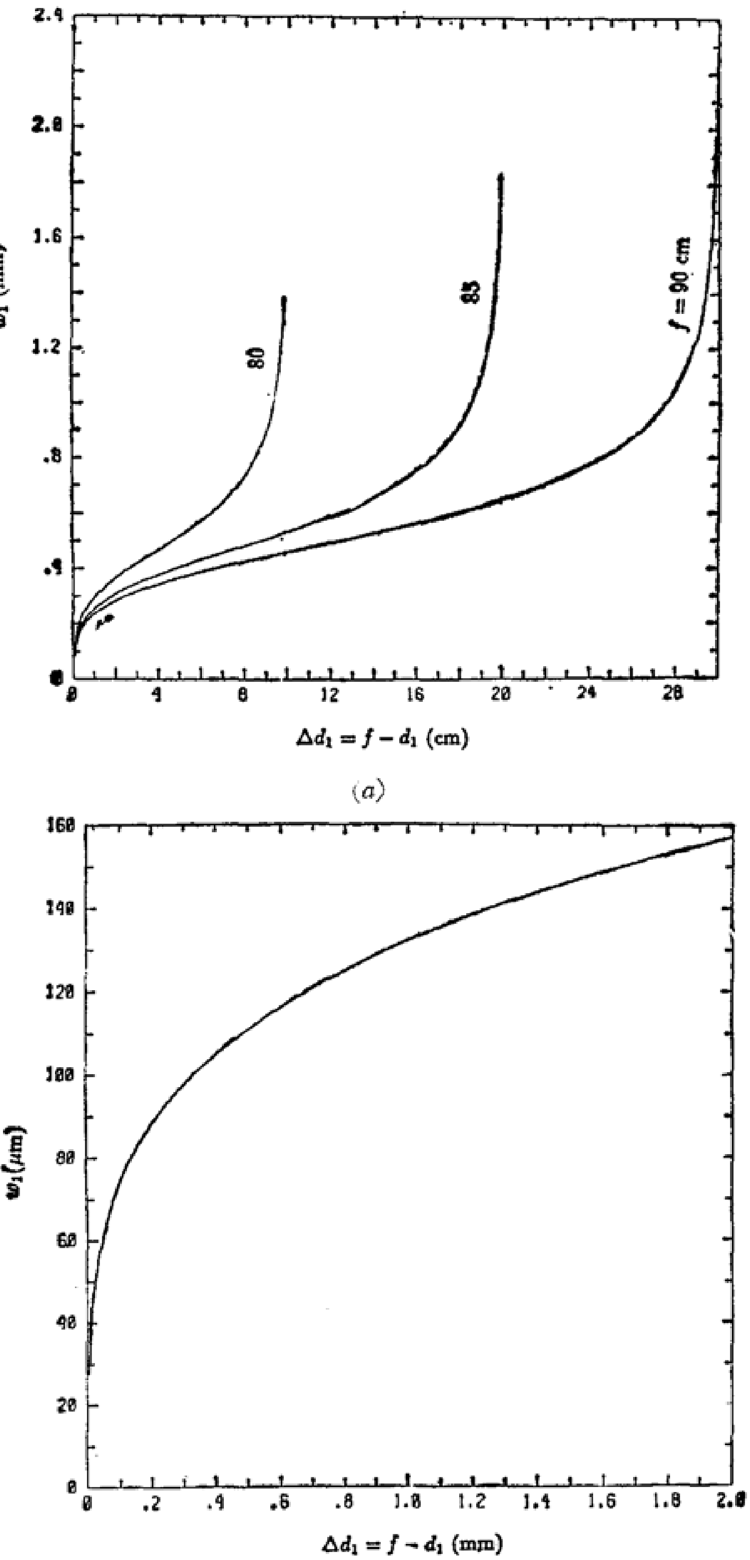

(a)

(b)

Fig. 5　Characteristics of the linear resonator in the first quadrant of stability, $f>d_1$ and d_2, $d_0=d_1+d_2=150$ cm $\Delta d_1=f-d_1$

(a) variations of the beam waist size w_1 vs. Δd_1;

(b) An enlargement of (b) with $f=90$ cm

with each other once d_1 passes $\frac{1}{2}d_0$. Thus, the variation of w_2 is just the reflection of the curves of w_1 in Fig. 5a at the corresponding inflection points. It is clear that near the center of the stable range, the beam waist size w_1 is fairly large. For longitudinal pump scheme, however, the pump beam size is required to be small ($w_p \leqslant 100\,\mu$m). Therefore, for a good match between the pump beam and intracavity laser beam volumes, one has to operate the resonator near its edge of the stable range. As shown in Fig. 5b the beam waist size w_1 changes very drastically from 50 μm to 100 μm over a small change of $d_1(\leqslant 0.4$ mm).Thus, practically such operation requires a fairly precise determination of d_1 and it is not easy to work with.

III. Experimental Results

Because of its nice properties, we chose to use a three-element resonator in the third quadrant. Its characteristics were verified experimentally. The experiments are performed with a $f=85$ mm thin lens and a total resonator length of $d_0=75$ cm. This is mainly due to the availability of the optics (the thin lens). The thin lens is anti-reflection coated at 1.054 μm to give a minimum intracavity loss. The Nd: phospate glass slab is placed near the plane mirror M_1 (Fig. 1) which is dichroic coated to give maximum reflection at 1.054 μm and maximum transmission at 514 nm. A CW argon ion laser at 514 mm (passing through mirror M_1) is used to longitudinally pump the Nd: glass slab. During the experiment, the pump laser power and beam size ($w_p\simeq 67$ μm) at the active medium are kept unchanged. The thin lens is monnted on a translator to allow variation of d_1.

We have measured the output beam divergence and laser power (through M_2) as d_1 varies. The experimentally observed lower and upper d_1 boundaries for lasing are 95.5 mm and 108.5 mm respectively. The theoretical stable range for the resonator employed is 85 mm$<d_1<$97.7 mm. Thus the observed stable range is shifted about 10 mm towards the larger d_1 values. Two causes contribute to such difference between the theoretical and the observed distance d_1. Firstly, in the physical laser resonator, because of the presence of the Nd:phosphate glass slab, the real distance between mirror M_1 and the intracavity thin lens $d_{1\text{Phys}}$ differs from d_1 of an empty resonator according to Eq. (9). The difference $d_{1\text{Phys}}-d_1$ is about 6.75 mm. Therefore, the observed distance should be larger than the d_1 of an empty resonator. The second cause to the observed larger $d_{1\text{Phys}}$ value is believed due to the thermal lensing effect[13]. With a thermal lens formed at the active medium, a new beam waist can be formed at the left side of the original beam waist. Thus, the position of mirror M_1 should be shifted left-wards, or the distance d_1 becomes larger.

Despite the observd, shifted stable range due to the above two causes, we can still compare the experimental data with theoretical calculations. Fig. 6 shows the theoretical and experimental beam divergences. Since the laser power is proportional to the overlap between the cross-section areas of the pump beam and the laser beam, we compare the laser output power (in arbitrary unit) to w_1^2, the square of the smaller beam waist size, in Fig. 7. In both Figs. 6 and 7, the abscissa is d_1-f for the

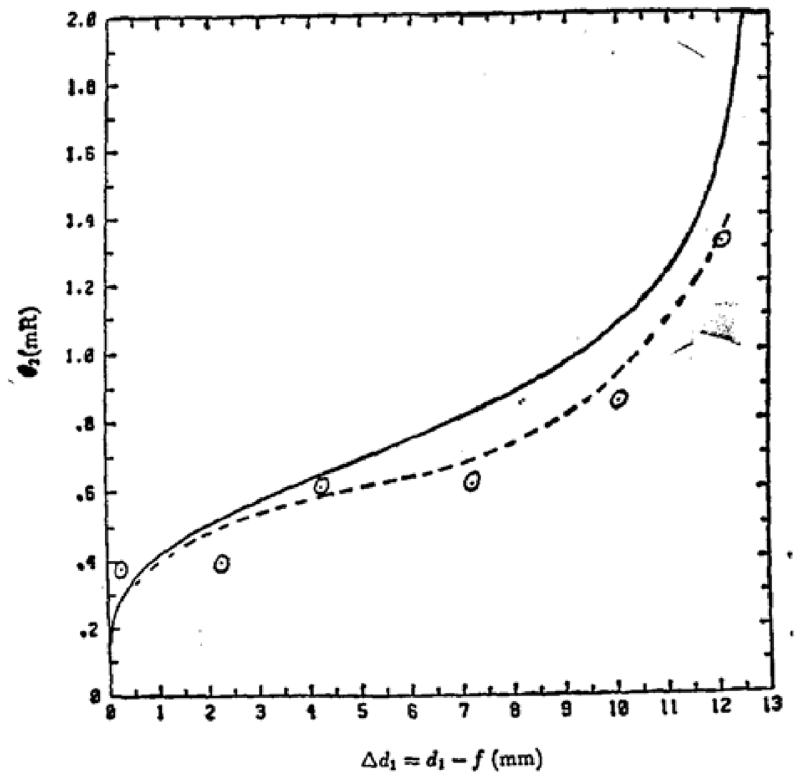

Fig. 6　The angle of divergence θ_2 from the output mirror. The solid line represents the theoretical calculation. The discrete points are the observed values. The broken line represents the changing tendency of experimental results

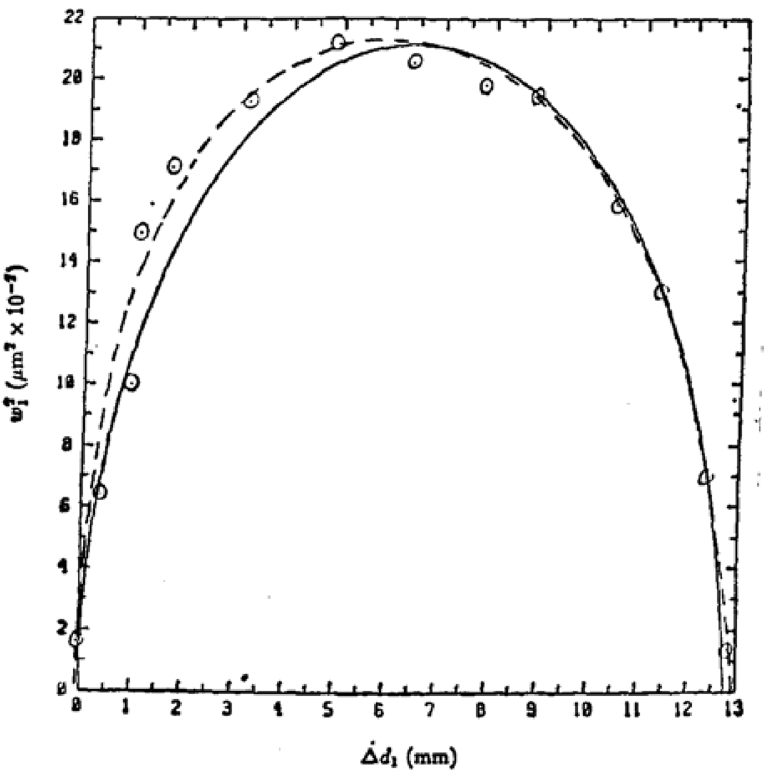

Fig. 7　The solid line is the theoretical calculation of the square of the small beam waist size w_1 against the change of d_1. The discrete points are the laser output power in arbitrary unit. The broken line represents the changing tendency of the experimental results

theoretical curves. The experimental data are plotted versus the increment of the physical distance and are fitted to match symmetrically to the theoretical stable range. The agreements between the theoretical calculations and the experimental data are generally good. From Fig. 7, we see that near the middle of the stable range, the beam size w_1 is maximum ($\sim 46\,\mu m$); this results in a maximum overlap of the pump and laser beams and consequently maximizes the pumping efficiency and the laser output power. At other d_{1Phys}, the intracavity laser beam size at the active medium reduces, resulting in a reduction of effective pumping and hence laser power. Near the edge of the stable range, the laser beam size becomes so small that the resultant gain is less than the intracavity loss and lasing stops. However, a quantitative analysis requires detail calculations involving the pump beam and the laser beam intensity distributions and that are not presented in this paper.

IV. Comparison Between Three Different Types of Resonators

In section III, we have discussed the characteristics of a linear three-element resonator. In this section we compare the linear resonator in both the first and the third quadrants with a third simple resonator, hemispherical resonator. In order to compare them on the same base, we choose two important resonator parameters to be nearly the same: the total resonator length d_0 and the smaller beam waist size w_1.

For a hemispherical resonator of length d_0 and radius of curvature of the spherical mirror R, the semi-confocal length z_0 of the resonator is[1]

$$z_0=\frac{\pi w_0^2}{\lambda}=[d_0(R-d_0)]^{1/2}. \tag{26}$$

Eq. (26) indicates that there are only two adjustable resonator parameters. For a fixed length d_0 and a concave mirror with radius of curvature R, the beam waist size w_0 is uniquely determined. In practical design R is discrete parameter and once it is chosen, it is fixed throughout the whole experiment. The only parameter left to control the beam waist size to match the end pumping beam size is d_0. We choose the radius of curvature of mirror R to be 150 cm and let d_0 change gradually to approach 150 cm; the variation of beam waist size w_0 is shown in Fig. 8*a*. It can be seen that w_0 reduces drastically in the small value region. However, in actively modelocking a laser, the total length d_0 sometimes needs to be changed to match the resonant frequency of the acousto-optic modulator. Such a change of d_0 could be as large as a few millimeters. Fig. 8*b*, enlarged from Fig. 8*a*, shows that a change of half millimeter in d_0 will cause a change of $70\,\mu m$ in the beam waist size w_0. Thus this type of resonator is quite difficult to work with.

For the three elemeet resonator in the first quadrant stability, it has one more parameter d_2 free to be adjusted to match the total resonator length d_0 with the resonant frequency of the acousto-optic modulator. Therefore, it is better than the hemispherical resonator. However, we have shown in Fig. 5*b* that, with $d_0=150$ cm

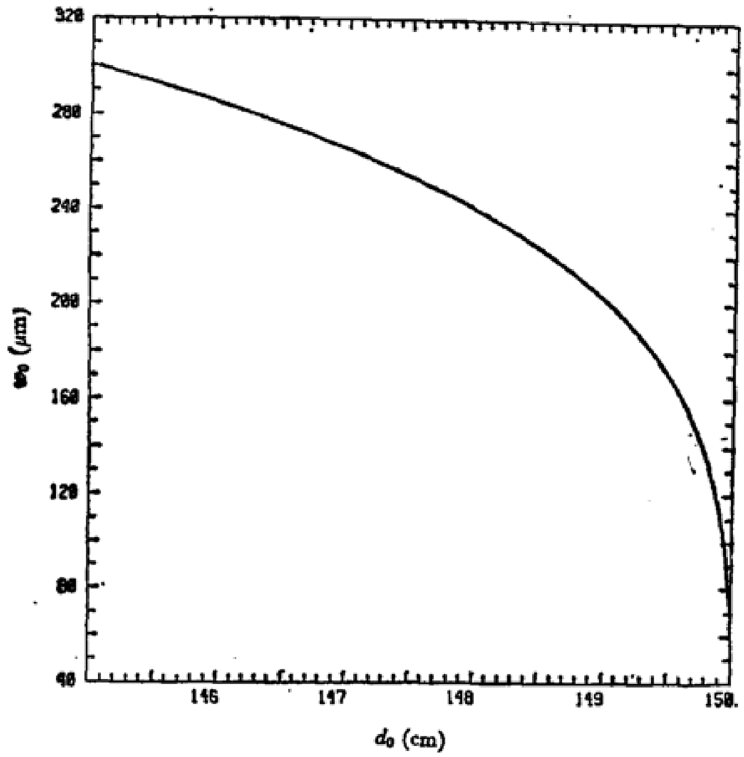

(a)

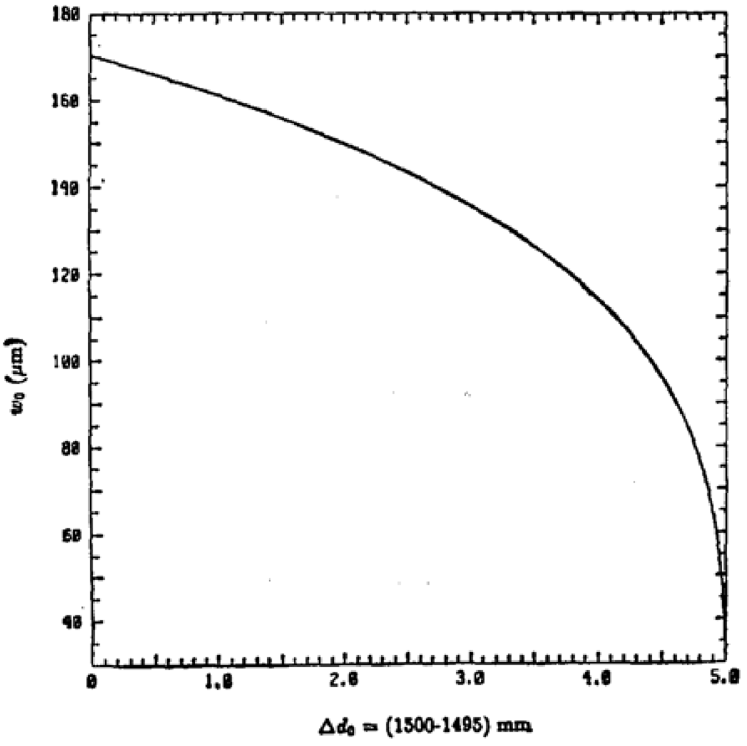

(b)

Fig. 8 The variation of beam waist size w_0 of the hemispherical resonator vs. d_0 or R_0

(a) R_0 is kept constant, 150 cm, and d_0 changes from 145 cm to 150 cm;

(b) An enlargement of the small w_0 region in (a)

and $f=90$ cm, a change of d_1 about 0.5 mm will cause a change of 80 μm of w_1. From the point of view of control sensitivity of the small beam waist size, the linear resonator in the first quadrant and the hemispherical resonator are quite comparable.

In section II, we discuss the effect of changing d_0 when f of the intracavity focusing lens is fixed for the linear resonator in the third quadrant. This type of resonator provides a much smoother change of beam waist size due to deviation of the actual resonator length from a designed one; thus the control demand on d_0 is much more relaxed and the resonator is much easier to work with. In the case of even larger change of d_0, such as in constructing a regenerative amplifier where the resonator length may be changed to result in a desired round trip time, such a flexibility of the three-element resonator will become much more important. In addition, for the linear resonator in the third quadrant, the smaller beam waist size w_1 has a maximum near the middle of stable range. Within half of the stable range of d_1, the value of w_1 changes only less than 7% of its maximum value, as shown in Fig. 3*a*. The variation of smaller beam waist size of this type of resonator is about two orders of magnitude smaller than the other two types.

We conclude that the linear resonator in the third quadrant not only provides a flexibility of changing the resonator length, but also has the feature of smooth variation of small beam waist size over a large range of the intracavity lens position. Such characteristics are desirable for the longitudinally pumped, actively mode-locked Nd: phosphate glass laser.

V. Applications to Other Variana Resonators

i) Linear resonator with an end concave mirror

In some cases one may prefer to have the intracavity beam waist located some distance away from the end mirror. For a Gaussian beam, the radius of curvature becomes finite at a distance z from the beam waist as given by[1]

$$R(z)=z\left[1+\frac{z_0^2}{z^2}\right], \qquad (27)$$

where $z_0=\frac{\pi\omega_0^2}{\lambda}$. When z is much greater than z_0, $R(z)$ is nearly equal to z. A concave mirror M_1' with $R=R(z)$ located at a distance z from the beam waist will match the wave front and form a stable resonator. This becomes a hemi-spherical resonator with an intracavity thin lens[9] as shown in Fig. 9. The other plane mirror M_2 could be replaced by another concave mirror at a proper distance; this corresponds to the case of Magni[6], i.e., the two concave mirrors with an intracavity thin lens. All the previous discussions of the resonator characteristics

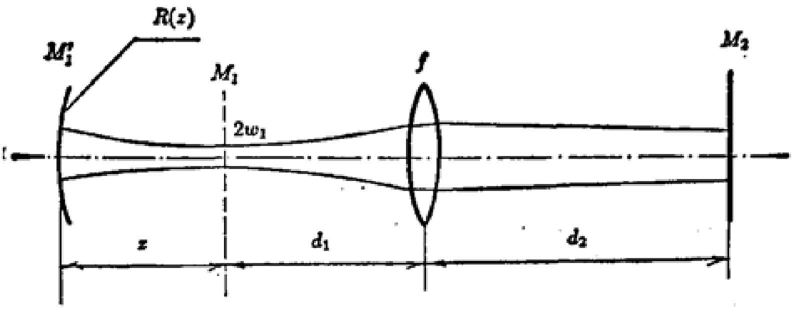

Fig. 9 Extended linear resonator with an end concave mirror. M_1', a concave mirror with radius of curvature $R(z)$, is put at a distance z from the beam waist w_1. M_2 is the end mirror of the original linear resonator. M_1 now represents only the position of the beam waist w_1

can be applied to this modified resonator, if one refers d_1 and/or d_2 as the distance between the thin focussing lens and the beam waist and bears in mind the corresponding change of the total resonator length.

ii) Folded resonator with a concave mirror

It is clear that the thin focussing lens can be replaced by a concave mirror with a radius of curvature R by which the ray is bended and forms a folded resonator. Except for the astigmatism introduced by the concave mirror which we do not consider here, the fundamental $ABCD$ matrix has the same form with f being replaced by $\frac{1}{2}R$. Thus, all the previous results remain the same with a substitution of $\frac{1}{2}R$ for f. The plane mirror of the folded resonator could be replaced by a concave mirror as discussed in the above section.

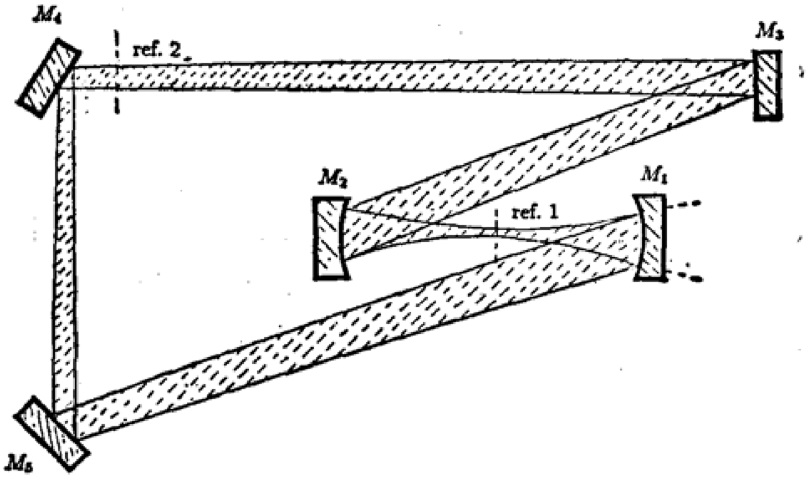

Fig. 10 The ring resonator. M_1, M_2–two concave mirrors with same radius of curvature R, M_3, M_4, M_5–plane mirrors. Ref. 1–first reference plane where the smaller beam waist at, Ref. 2–second reference plane where the larger beam waist at

iii) Ring resonator

Fig. 10 shows the schematic of a ring resonator. Physically it is clear that there is a small beam waist at the middle between the two concave mirrors and a large beam waist at a plane half round trip resonator length from the small one. When the reference plane is chosen at the middle between the two concave mirrors, the round trip $ABCD$ matrix is then given by

$$\begin{pmatrix} A' & B' \\ C' & D' \end{pmatrix}=\begin{pmatrix} 1 & \frac{d_1'}{2} \\ 0 & 1 \end{pmatrix}\begin{pmatrix} 1 & 0 \\ -\frac{2}{R} & 1 \end{pmatrix}\begin{pmatrix} 1 & d_2' \\ 0 & 1 \end{pmatrix}\begin{pmatrix} 1 & 0 \\ -\frac{2}{R} & 1 \end{pmatrix}\begin{pmatrix} 1 & \frac{d_1'}{2} \\ 0 & 1 \end{pmatrix}$$

$$=\begin{pmatrix} 1-\frac{2d_1'}{R}-\frac{2d_2'}{R}+\frac{2d_1'd_2'}{R^2} & d_1'+d_2'-\frac{2d_1'd_2'}{R}-\frac{d_1'^2}{R}+\frac{d_1'^2d_2'}{R^2} \\ -\frac{4}{R}+\frac{4d_2'}{R^2} & 1-\frac{2d_1'}{R}-\frac{2d_2'}{R}+\frac{2d_1'd_2'}{R^2} \end{pmatrix}. \tag{28}$$

Comparing Eqs. (1) and (28), one finds that with interchanges $d_1'\to 2d_1$, $d_2'\to 2d_2$, and $\frac{R}{2}\to f$, the matrix (25) is identical to the matrix (1). Thus, the characteristics of this type of ring resonator is the same as that of the linear resonator discussed in section II.

There is another way to view the similarity between the ring resonator and the folded resonator. If two flat mirrors are put at the two beam waists with a normal reflection respectively, one changes the ring resonator into a folded resonator. The only difference is that the light wave passes through the two beam waists in the ring resonator, forming a traveling wave oscillation, and the light wave is reflected backwards at the two beam waists of the folded resonator forming a standing wave oscillation. Hawever, as regard to the resonator characteristics such as the stability condition and beam waist size and their variations vs. different parameters, the two resonators are equivalent.

VI. Conclusion

Continuous wave mode-locked Nd: phosphate glass laser requires special resonator design since Nd: phosphate glass has low thermal conductivity and damage threshold. We have studied the characteristics of a three-element optical resonator under the constraint of a fixed resonator length. By adjusting the position of the intracavity thin lens, sizes of two beam waists can be varied. We show that in the third quadrant regime, i.e., $f<d_1$ and d_2, the stable range is about a few centimeters. Near the middle of the stable range, the smaller beam waist is at maximum with a size w_{1max} easily to change over a large range by properly choosing the focal length of the intracavity thin lens. Analytical formulas of resonator parameters for optimum operation regime are given for either fixed d_0 or a fixed d_2. Experimental results agree well with theoretical predictions. A comparison with a conventional hemispherical resonator shows that such a three-element resonator offers a freedom of adjusting the total resonator length and requires much less stringent control of positions of resonator elements, which is desirable for the longitudinally pumped, actively mode-locked Nd: phosphate glass laser. The analysis can also be applied or extended to folded resonator and ring resonator and may be useful for the design of any end-pumped and mode-locked resonator with three elements.

Acknowledgement

We would like to thank P.-T. Ho and E. A. Chauchard for discussions. Thanks are due to Mr. Zhou Zhong Yi and Mr. Chen Tao Lue for the early stage of discussion and calculation in Shanghai Institute of Optrcs & Fine Mechanics.

References

[1] H. Kogelnik and T. Li; *Proc. IEEE*, 1966, **54**, No. 10 (Oct), 1312~1329.
[2] H. Kogelnik; *Bell Syst. Tech. J.*, 1965, **44**, 455.
[3] S. A. Tuccio, F. C. Strome, *Jr.*; *Appl. Opt.*, 1972, **11**, No. 1 (Jan), 64~73.
[4] H. W. Kogelnik *et al.*; *IEEE J. Q. E.*, 1972, **QE-8**, No. 3 (Mar), 373~379.
[5] H. P. Kortz, R. Iffländer, and H. Weber; *Appl. Opt.*, 1981, **20**, No. 23 (Dec), 4124~4134.
[6] V. Magni; *Appl. Opt.*, 1986, **25**, No. 1 (Jan), 107~117.
[7] S. A. Strobel *et al.*; *Appl. Phys. Lett.*, 1984, **45**, No. 11 ((Dec), 1171~1173.
[8] L. Yan *et al.*; *Opt. Lett.*, 1986, **11**, No. 8 (Aug), 502~503.
[9] O. G.Peterson, *et al.*; *Appl. Phys. Lett.*, 1970, **17**, No. 6 (Sep), 245~247.
[10] J. D. Ling; "*Trnasformation of Wave Front on the Internal Lens of Resonator*", (China Laser III Conference Canton, China, 1978 Summer).
[11] G. Herziger and H. Weber; *Appl. Opt.*, 1984, **23**, No. 10 (May), 1450~1452.
[12] Ayariv; "*Quantum Electronics*",2nd ed; (John Wiley and Sons, New York, 1975).
[13] Li Yan; "*Generation of Ultrashort Laser Pulses from Neodymium glass Oscillator and Regenerative Amplifier*", (University of Maryland, Ph. D. dissertation, 1989).
[14] W. Koechner; "*Solid-State Laser Engineering*", (Springer-Verlag, Berlin, 1976).

连续波锁模掺钕磷酸盐玻璃激光器光学谐振腔的分析

凌君达　L. Yan　李齐相
(马里兰大学·电气工程系，美国)
(收稿日期：1990年2月6日)

提　　要

由于 Nd:磷酸盐玻璃的热导率和破坏阀值都比较低，故连续波锈模钕磷酸盐玻璃激光器要求其谐振腔有特殊的设计。本文在谐振腔长度固定的限制下，分析了三元件式谐振腔的特性，并且讨论了连续波主动锁模 Nd:磷酸盐玻璃激光器光学谐振腔的设计。我们讨论了在不同参量范围下谐振腔的稳定性范围和特性，并且阐明了有关的最佳参数的范围。给出了谐振腔最佳运转区参数的解析表达式。实验结果与理论预测符合得很好。这个解析式对设计三元件或多元件的任何端面泵浦和锁模谐振腔是很有用的。
关键词：Nd:磷酸盐玻璃激光器；三元件式谐振腔；主动锁模激光器。